Stroboscopic Qubit Measurement with Squeezed Illumination

A. Eddins,[1,2] S. Schreppler,[1,2] D. M. Toyli,[1,2] L. S. Martin,[1,2] S. Hacohen-Gourgy,[1,2] L. C. G. Govia,[3,4]
H. Ribeiro,[3] A. A. Clerk,[3,4] and I. Siddiqi[1,2]

[1]*Quantum Nanoelectronics Laboratory, Department of Physics, University of California, Berkeley, California 94720, USA*
[2]*Center for Quantum Coherent Science, University of California, Berkeley, California 94720, USA*
[3]*Department of Physics, McGill University, Montréal, Québec H3A 2T8, Canada*
[4]*Institute for Molecular Engineering, University of Chicago, Chicago, Illinois 60637, USA*

Microwave squeezing represents the ultimate sensitivity frontier for superconducting qubit measurement. However, measurement enhancement has remained elusive, in part because integration with standard dispersive readout pollutes the signal channel with antisqueezed noise. Here we induce a stroboscopic light-matter coupling with superior squeezing compatibility, and observe an increase in the final signal-to-noise ratio of 24%. Squeezing the orthogonal phase slows measurement-induced dephasing by a factor of 1.8. This scheme provides a means to the practical application of squeezing for qubit measurement.

Electromagnetic quadrature squeezing is the reduction below vacuum noise of fluctuations in, for example, either the $\sin(\omega t)$ or $\cos(\omega t)$ component of the electric field. Besides being of fundamental interest as nonclassical states of light, squeezed states can enable faster measurements in cases where field intensity is limited, utilizing multiparticle quantum correlations to encode more information per photon, which manifests as a reduction in noise. Optimally applied squeezing can result in Heisenberg-limited scaling, wherein the signal-to-noise power ratio (SNR) scales not as the number of measurement photons but as the square. The development of squeezing at optical frequencies has a long history [1] leading to a range of recent applications such as gravitational wave detection [2,3]. Squeezing of microwave-frequency fields using superconducting amplifiers [4–6] has surged as a topic of interest in the modern contexts of circuit quantum electrodynamics and dark matter detection [7] given the ability to couple squeezed fields to low-dimensional quantum systems such as superconducting qubits [8–10], optomechanical circuits [11,12], or spin ensembles [13].

Despite interest in using squeezed microwaves for superconducting qubit measurement, experimental realization has remained elusive. A major challenge is that the dispersive coupling central to standard readout techniques rotates squeezing out of, and antisqueezing into, the signal quadrature, limiting SNR improvement outside of certain restrictive parameter regimes [14]. Proposals to fully exploit squeezing for qubit measurement have been suggested, however with the need for more complex circuit architectures involving multiple readout modes [15,16] or a fundamentally different longitudinal qubit-cavity coupling [17]. In this Letter, we employ a stroboscopic longitudinal coupling [18] compatible with large amounts of squeezing and standard qubit designs to harness input squeezing for qubit measurement. Stroboscopic techniques have been intensely studied in "backaction evading" optomechanical systems [19–21], but they have not been combined with injected squeezing.

Stroboscopic measurement occurs within a rotating frame in which the terms which limit the benefit of squeezing for conventional dispersive readout are suppressed. The scheme consists of a qubit Rabi-oscillating at frequency Ω_R coupled to a cavity driven by sideband tones at $\omega_c \pm \Omega_R$. The interaction-picture Hamiltonian is $\hat{H}_I = \chi\hat{\sigma}_z a^\dagger a + (\Omega_R/2)\hat{\sigma}_x + \hat{H}_{\rm sb}$, where $\hat{H}_{\rm sb}$ describes the sideband drives. Decomposing the resulting cavity field into its classical and quantum parts, $\hat{a} \to 2\bar{a}_0 \cos(\Omega_R t) + \hat{d}$, and transforming to the Rabi-driven qubit frame yields

$$\hat{H}_R = \chi\bar{a}_0\hat{\sigma}_z^R(\hat{d} + \hat{d}^\dagger) + (e^{i\Omega_R t}\hat{A} + e^{i2\Omega_R t}\hat{B} + {\rm H.c.}). \quad (1)$$

The first term of Eq. (1) describes a resonant longitudinal and quantum nondemolition (QND) coupling between the qubit and one quadrature of the cavity field. The measured qubit observable $\hat{\sigma}_z^R$ has an explicit time dependence in the original interaction picture, $\hat{\sigma}_z^R \to \cos(\Omega_R t)\hat{\sigma}_z - \sin(\Omega_R t)\hat{\sigma}_y$, making it analogous to a quadrature operator of a harmonic oscillator. The remaining terms in Eq. (1), discussed explicitly in the Supplemental Material [22], represent deviations from the ideal QND coupling, including terms that would cause an unwanted rotation of any input squeezing. These deleterious terms are rapidly oscillating, and hence are strongly suppressed if $\Omega_R \gg \kappa, \chi$. In contrast, there is no such suppression in a standard dispersive measurement, as such effects are resonant.

To combine squeezing and stroboscopic measurement experimentally, we embed a 3D-transmon qubit [25] in a series configuration of two Josephson parametric amplifiers

(JPAs) squeezing independent phase-space quadratures [Fig. 1(a)]. Several recent experiments not involving superconducting qubits have utilized similar configurations of superconducting amplifiers [13,26,27], which have been predicted to exhibit Heisenberg-like scaling in some regimes [28]. The qubit ($\omega_q/2\pi = 3.898$ GHz) is coupled to a two-port superconducting waveguide cavity ($\omega_c/2\pi = 6.694$ GHz) with a dispersive interaction strength $\chi/2\pi = 0.73$ MHz.

Into the weakly coupled port ($\kappa_{\mathrm{weak}}/2\pi \leq \kappa_{\mathrm{int}}/2\pi \sim 10$ kHz), we inject coherent qubit and cavity drives to generate stroboscopic measurement. The drive resonant with the qubit induces Rabi oscillations about $\hat{\sigma}_x$ at $\Omega_R/2\pi = 40$ MHz exhibiting characteristic lifetimes $T_{\mathrm{Rabi}} \sim 20$–$30$ μs. Concurrently, a pair of cavity drives at frequencies $\omega_c \pm \Omega_R$, equivalent to a drive at ω_c modulated at $2\Omega_R$, stroboscopically probes the qubit state. Varying the relative phase of these two tones varies the timing of the modulation relative to the Rabi oscillations such that we can choose to measure any combination of $\hat{\sigma}_y^R$ and $\hat{\sigma}_z^R$ [Fig. 1(b)]; for all measurements presented here we choose to measure $\hat{\sigma}_z^R$, equivalent to a $\hat{\sigma}_z$ measurement in the absence of a Rabi drive ($\Omega_R \to 0$). The measurement interaction [Eq. (1)] displaces the cavity output field in phase space by $\pm 2\bar{a}_0 \chi/\kappa$ [18,22], in contrast to dispersive measurements which rotate the output field through the angle $\pm \arctan(2\chi/\kappa)$, or twice this angle for reflection measurements [Fig. 1(c)]. For all measurements shown below, we choose $\bar{a}_0 = 0.35$, corresponding to a mean photon number of 0.5 in the coherent part of the cavity field.

Into the strongly coupled cavity port ($\kappa_{\mathrm{strong}}/2\pi = 5.9$ MHz), we inject squeezed vacuum at ω_c produced by the first JPA, labeled SQZ in Fig. 1(a). Keeping $\kappa_{\mathrm{strong}} \gg \kappa_{\mathrm{weak}}$ ensures that unsqueezed vacuum fluctuations incident to the weakly coupled port can be neglected and do not spoil the intracavity squeezing. We deliberately designed the squeezer to have a bandwidth smaller than Ω_R

($\kappa_{\mathrm{SQZ}}/2\pi = 26$ MHz when the amplifier is off) to avoid generating significant squeezed noise power at the frequencies of the two measurement tones, similar to narrow-band squeezers used in previous works [9]. We use a vector network analyzer to separately measure the phase-preserving squeezer gain, G_{SQZ}, from which we infer the amount of squeezing generated at this JPA. The resulting intracavity squeezed state is displaced in phase space from the origin along the I quadrature by the stroboscopic measurement interaction [Fig. 1(a)]; we can freely adjust the squeezer pump phase to orient the squeezing angle Φ in phase space parallel ($\Phi = 0$) or perpendicular ($\Phi = \pi/2$) to this signal.

In order for the squeezing of vacuum fluctuations to have a significant effect on the SNR achieved at room temperature, the signal must be amplified with high efficiency. The signal travels from the cavity via the strongly coupled port to a series of two superconducting amplifiers: a second JPA, labeled AMP in Fig. 1(a), followed by a Josephson traveling wave parametric amplifier (JTWPA). The JTWPA functions as a high dynamic range amplifier ($P_{-1\,\mathrm{dB}} \sim -100$ dBm at 20 dB gain) that lowers the noise temperature of the measurement chain, referred to the JTWPA input, to be less than 1 K [29]. This permits operating the second JPA at modest gain less than 20 dB, such that nonlinearities do not degrade the efficiency of the phase-sensitive amplification [13,30].

This hardware configuration enables control via squeezing of the speed at which the cavity field acquires information about the qubit, which is reflected in the rate of measurement backaction. With the signal in the field quadrature I, backaction is exerted on the qubit by fluctuations of the conjugate variable Q. When no squeezing is applied, these fluctuations are those of the electromagnetic vacuum, which has a variance of $1/4$ in all phase-space directions, and the resulting dephasing rate is given by $\Gamma_\varphi = 8\bar{a}_0^2 \chi^2/\kappa$ [18]. The observed decay of a
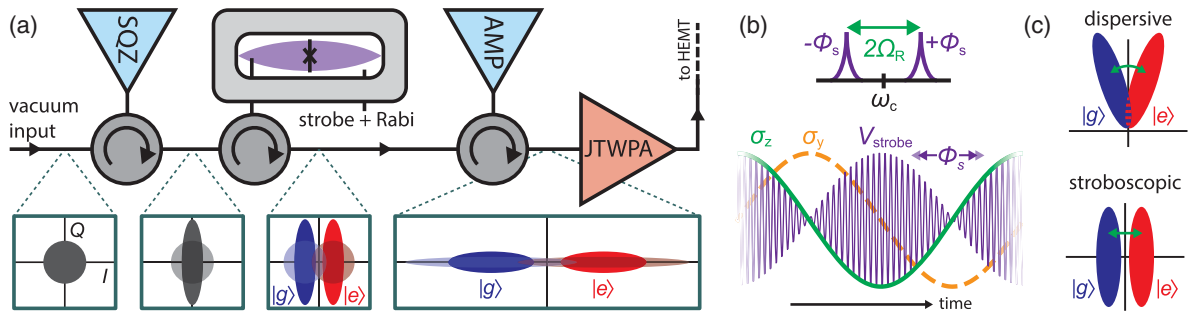

FIG. 1. (a) Simplified experimental setup. A first Josephson parametric amplifier (SQZ) injects squeezed vacuum into a superconducting cavity containing a qubit. The qubit is Rabi-driven at Ω_R about $\hat{\sigma}_x$ and measured by two tones at frequencies $\omega_c \pm \Omega_R$, resulting in a qubit-state-dependent displacement of the squeezed field in phase space. A second Josephson parametric amplifier (AMP) followed by a Josephson traveling wave parametric amplifier (JTWPA) perform phase-sensitive and phase-preserving amplification, respectively, of the output signal. Insets show phase-space representations of an ideal lossless measurement with (solid) and without (shaded) squeezing. (b) We choose the two tones' relative phase ϕ_s such that the envelope of the resulting measurement field is in phase with $\hat{\sigma}_z$. (c) Whereas dispersive readout rotates the output field in phase space, stroboscopic readout displaces the output field, providing greater potential for enhancement by squeezing.

Ramsey oscillation occurring during a measurement of a chosen strength indicates a steady-state dephasing rate $\Gamma_\varphi = 0.54(1)\ \mu s^{-1}$ [Fig. 2(a)]. We compare to this baseline the Γ_φ seen when fluctuations in the measurement field are squeezed. Changing the amplitude of the JPA pump controls the amount of squeezing, while changing the pump phase rotates the squeezing relative to I and Q. With the pump amplitude fixed such that $G_{SQZ} = 3.8$ dB, squeezing along the backaction quadrature Q ($\Phi = \pi/2$) slows down Γ_φ by a factor of 1.8, indicating 2.5 dB of squeezing inside the cavity, and also amplifies fluctuations in the signal quadrature I, reducing the rate at which qubit state information leaves the cavity. The ability to slow a qubit measurement with squeezing is desirable in circumstances where a measurement occurs as an unwanted side effect of a quantum operation, and has been proposed as a tool for realizing high-fidelity multiqubit gates [31]. Conversely, squeezing along I ($\Phi = 0$) increases Γ_φ by a factor of 3.9 (5.9 dB) and increases the output field SNR. We model the dephasing rate as
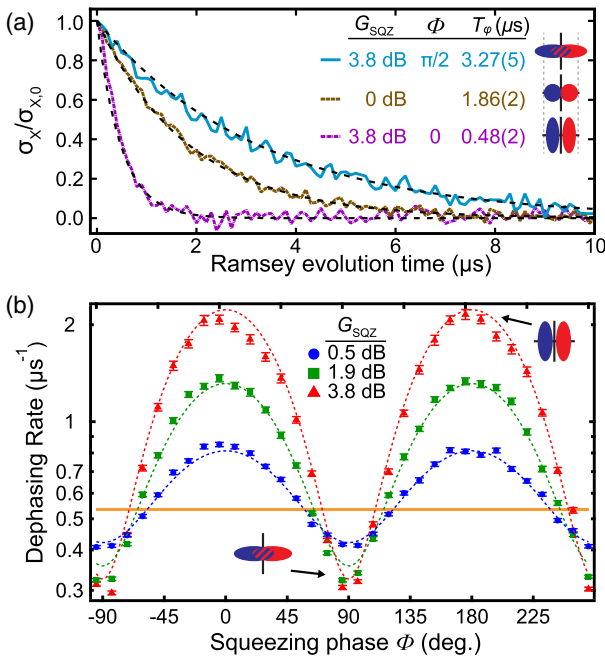

(a)

(b)

FIG. 2. (a) Ensemble-averaged Ramsey decay traces during a stroboscopic $\hat{\sigma}_z$ measurement with no squeezing (brown) or with squeezing in phase (purple) or out of phase (cyan) with the measurement signal. Each trace is normalized by its initial $t = 0$ value, $\sigma_{x,0}$. Here the squeezer is pumped for 3.8 dB of phase-preserving gain as determined by Lorentzian fits of S_{21} vs probe frequency. (b) Steady-state dephasing rates $\Gamma_\varphi = 1/T_\varphi$ were acquired via Ramsey measurements as in (a), repeated for a range of phases and squeezer gains. The orange horizontal band is the dephasing rate with the squeezer off. Error bars, including the width of the horizontal band, represent statistical fit uncertainties. The dashed curves are the results of a joint fit of all data in Figs. 2(b) and 3(b).
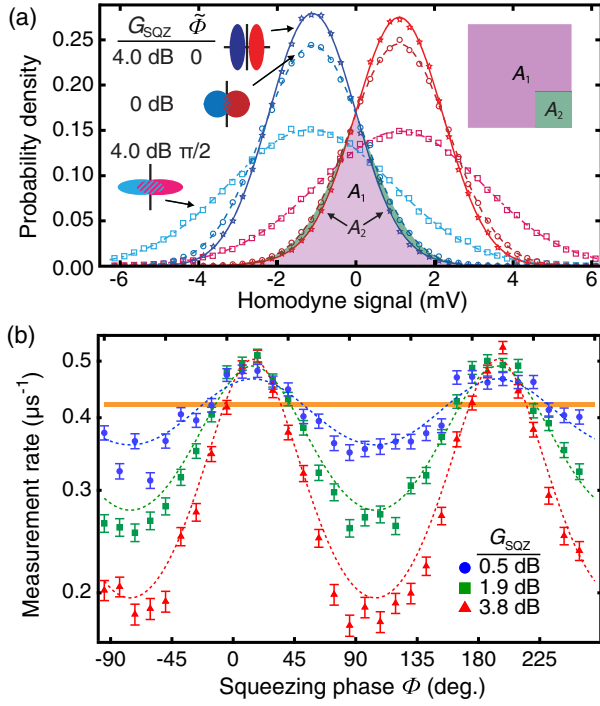
$$\Gamma_\varphi = \Gamma_{\varphi,vac} \frac{\Delta_Q^2}{1/4} = \Gamma_{\varphi,vac}[1 + 2\epsilon_{in}(N + M\cos 2\Phi)], \quad (2)$$

where Δ_Q^2 is the field variance in the Q quadrature inside the cavity, $1 - \epsilon_{in}$ is the loss between the squeezer and qubit, and the squeezing parameters N and M [32] are defined such that the variance of the amplified (squeezed) quadrature is $(1/2 + N \pm M)/2$ at the squeezer output. We measure loss in the JPA and calculate a negligible effect on squeezing, so we model the JPA as producing an ideal squeezed state with $M = \sqrt{N(N+1)}$ and $N = G_{SQZ} - 1$ both fixed by measurements of G_{SQZ}. A fit to the dephasing times shown in Fig. 2(b), jointly fit with the corresponding measurement times as discussed below, determines the input efficiency $\epsilon_{in} = 0.48$.

For a given squeezer setting, the squeezing-induced increase (decrease) in Γ_φ should correspond to an increase (decrease) in the SNR at our room-temperature homodyne detection setup. As in the dephasing rate study, we begin by determining a baseline with the squeezer off. We repeatedly prepare the qubit in either the ground or excited state and generate histograms of the results of stroboscopic measurements, indicated by circles in Fig. 3(a). We calculate the SNR = $[2(\bar{V}_e - \bar{V}_g)/(\sigma_e + \sigma_g)]^2$ from the mean separation and widths of the histogram distributions. For a given $\Gamma_{\varphi,vac}$ produced by an unsqueezed steady-state measurement field at the qubit, SNR = $8\Gamma_{\varphi,vac}T_{int}\epsilon_{out}$, where T_{int} is the integration time and ϵ_{out} is the efficiency of the measurement chain downstream of the qubit. From the slope of SNR vs T_{int} we infer the steady-state measurement rate $\Gamma_{meas,vac}$ and the output efficiency $\epsilon_{out} = \Gamma_{meas,vac}/2\Gamma_{\varphi,vac} = 0.38$.

We repeat these measurements while squeezing or antisqueezing the noise in the signal quadrature, producing the histograms indicated by stars and squares, respectively, in Fig. 3(a). With $G_{SQZ} = 4.0$ dB, we observe narrowed histograms with reduced overlap area; from the slope of SNR(t) we determine a 24% increase in Γ_{meas} from $0.41(1)\ \mu s^{-1}$ without squeezing to $0.51(1)\ \mu s^{-1}$ with squeezing. A separate set of measurements display the dependence of Γ_{meas} on squeezing amount and phase, as shown in Fig. 3(b). As the SNR and thus Γ_{meas} should vary inversely with variance Δ_I^2 at the end of the measurement chain, we fit the data with the expression

$$\Gamma_{meas} = \Gamma_{meas,vac} \frac{1/4}{\Delta_I^2}$$
$$= \Gamma_{meas,vac}[1 + 2\epsilon_{in}\epsilon_{out}(N - M\cos 2\tilde{\Phi})]^{-1}. \quad (3)$$

The free parameters in the joint fit of Γ_φ and Γ_{meas} are $\epsilon_{in} = 0.48$, a global phase, and an offset $\delta = \Phi - \tilde{\Phi} = 14°$ capturing imperfect alignment of AMP with the signal quadrature, which shifts $\Gamma_{meas}(\Phi)$ but not $\Gamma_\varphi(\Phi)$. We fix $\Gamma_{\varphi,vac}$, $\Gamma_{meas,vac}$, and ϵ_{out} at the values found with no

FIG. 4. The overall measurement efficiency $\eta(\Phi)$ is shown for several values of G_{SQZ}. The data and fits are computed from the corresponding elements in Figs. 2(b) and 3(b). We attribute the asymmetry about phases where Φ is a multiple of $\pi/2$ to misalignment of the signal quadrature with the amplification quadrature of the second JPA. A small increase in η above ϵ_{out} can be resolved at low squeezer gain near $\Phi = \pi/2$.

FIG. 3. (a) Data points are normalized histograms of the mean homodyne voltage integrated for 1.8 μs conditioned on preparing the qubit in the ground (blue colors) or excited (red colors) states. Curves are Gaussian fits. Measurements were repeated with squeezed (stars, solid), unsqueezed (circles, dashed) and anti-squeezed (squares, dot-dashed) noise. Fits of data conditioned on excited-state preparation include a small second Gaussian to capture ground-state population ($\lesssim 2\%$) attributable to qubit relaxation before and during the Rabi ramp-up. The overlap area is smaller with squeezing (A_1) than without squeezing ($A_1 + A_2$). (b) The measurement rate Γ_{meas} is determined for multiple phases and amounts of squeezing. The orange horizontal band is Γ_{meas} with SQZ off. Error bars, including the width of the horizontal band, are standard errors of fits of SNR(t). The dashed curves are results of a joint fit of all the data in Figs. 2(b) and 3(b) with free parameters ϵ_{in}, δ, and a global phase.

squeezing. As expected, $\Gamma_{\text{meas}}(\Phi)$ is π-periodic, with phases maximizing Γ_{meas} close to those maximizing Γ_φ.

Comparing Γ_φ and Γ_{meas} reveals that, despite the intrinsic fragility of squeezing in the presence of loss, it is also possible for injected squeezing to improve the measurement efficiency η in a lossy environment. Here we define $\eta = \Gamma_{\text{meas}}/2\Gamma_\varphi$ such that for perfect efficiency $\eta = 1$. With the squeezer off, the efficiency reduces to $\eta_{\text{vac}} = \epsilon_{\text{out}}$, set by loss and added noise in the measurement chain downstream of the qubit. With the squeezer on, η depends also on ϵ_{in}, according to

$$\eta = \frac{\Gamma_{\text{meas}}}{2\Gamma_\varphi} = \eta_{\text{vac}} \frac{\Gamma_{\varphi,\text{vac}}}{\Gamma_\varphi} \frac{\Gamma_{\text{meas}}}{\Gamma_{\text{meas,vac}}}, \qquad (4)$$

where the ratios are manifest in equations (2) and (3), respectively. Figure 4 shows $\eta(\Phi)$, calculated by dividing Fig. 3(b) by Fig. 2(b); near $\Phi = \pi/2$, η increases from 0.38(1) to 0.42(1). The increase can be understood by comparing the
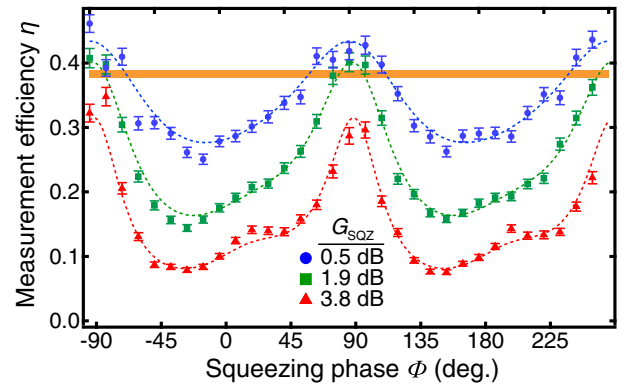
effect of the output loss $1 - \epsilon_{\text{out}}$ on SNR with and without squeezing. In both cases, the mean signal size at the cavity output is the same, and this signal is attenuated by the factor $1 - \epsilon_{\text{out}}$. Without squeezing, the vacuum fluctuations in the signal quadrature I are unaffected by the loss, so the SNR is reduced by $1 - \epsilon_{\text{out}}$. In contrast, squeezing along Q ($\Phi = \pi/2$) injects amplified noise in I which does get attenuated, partially canceling the effect of loss on SNR. Although the initial SNR leaving the cavity is lower in this case, so is the measurement backaction, as the Q quadrature is squeezed. Thus, at the cost of decreasing Γ_{meas}, η can be increased, with greater enhancement seen in systems with $\epsilon_{\text{in}} \gg \epsilon_{\text{out}}$. For example, $\eta > 50\%$ with only phase-preserving amplification of the signal is possible. Recently, a similar technique was demonstrated using squeezing to increase the robustness of optical cat-states [33]. The orthogonal case ($\Phi = 0$) has the reverse effect, increasing Γ_{meas} and decreasing η, with more speed-up in systems with high ϵ_{out}.

In summary, this work demonstrates that input squeezing can reduce the noise in measurements of standard superconducting qubits, and can also slow a measurement process and its associated dephasing. In general, the photon number is bounded by the nonlinearity of the qubit-field interaction, so maximizing information per photon is useful for, e.g., speeding up a quantum algorithm in which measurement is a bottleneck. Similarly, by squeezing the other quadrature, it may be possible to reduce the necessary wait time for cavity depopulation at the end of a measurement. A natural next step is to implement our techniques in a system highly optimized for efficiency [34], possibly incorporating ongoing development of superconducting circulators or on-chip amplifiers [35–38]. As squeezing cannot improve the SNR by more than a factor of $(1 - \epsilon_{\text{out}})^{-1}$, here equal to 1.6, efficiency improvements would better leverage the large amounts of microwave squeezing, exceeding 12 dB [6],

produced to date. Absent loss, our experimental setup is predicted to effectively utilize up to 16 dB of squeezing [22]. Complementary studies may explore the limits of stroboscopic readout speed by optimizing couplings or by increasing Ω_R to further suppress counter-rotating terms. The latter may be facilitated by modern high-anharmonicity qubit designs such as the C-shunt flux qubit [39]. Finally, it would be useful to investigate transient effects in the presence of squeezing, which are of increasing importance for shorter measurement times. Here stroboscopic or other longitudinal readout schemes may be advantageous even without squeezing, as the cavity-field ring-up and ring-down trajectories are expected to follow straight lines in phase space, in contrast to the circuitous short-time response of dispersive measurements [17].

[1] U. L. Andersen, T. Gehring, C. Marquardt, and G. Leuchs, Phys. Scr. **91**, 053001 (2016).
[2] J. Abadie *et al.*, Nat. Phys. **7**, 962 (2011).
[3] J. Aasi *et al.*, Nat. Photonics **7**, 613 (2013).
[4] B. Yurke, P. G. Kaminsky, R. E. Miller, E. A. Whittaker, A. D. Smith, A. H. Silver, and R. W. Simon, Phys. Rev. Lett. **60**, 764 (1988).
[5] M. A. Castellanos-Beltran, K. D. Irwin, G. C. Hilton, L. R. Vale, and K. W. Lehnert, Nat. Phys. **4**, 929 (2008).
[6] C. Eichler, Y. Salathe, J. Mlynek, S. Schmidt, and A. Wallraff, Phys. Rev. Lett. **113**, 110502 (2014).
[7] H. Zheng, M. Silveri, R. T. Brierley, S. M. Girvin, and K. W. Lehnert, arXiv:1607.02529.
[8] K. W. Murch, S. J. Weber, K. M. Beck, E. Ginossar, and I. Siddiqi, Nature (London) **499**, 62 (2013).
[9] D. M. Toyli, A. W. Eddins, S. Boutin, S. Puri, D. Hover, V. Bolkhovsky, W. D. Oliver, A. Blais, and I. Siddiqi, Phys. Rev. X **6**, 031004 (2016).
[10] S. Kono, Y. Masuyama, T. Ishikawa, Y. Tabuchi, R. Yamazaki, K. Usami, K. Koshino, and Y. Nakamura, Phys. Rev. Lett. **119**, 023602 (2017).
[11] J. B. Clark, F. Lecocq, R. W. Simmonds, J. Aumentado, and J. D. Teufel, Nat. Phys. **12**, 683 (2016).
[12] J. B. Clark, F. Lecocq, R. W. Simmonds, J. Aumentado, and J. D. Teufel, Nature (London) **541**, 191 (2017).
[13] A. Bienfait, P. Campagne-Ibarcq, A. Holm-Kiilerich, X. Zhou, S. Probst, J. J. Pla, T. Schenkel, D. Vion, D. Esteve, J. J. L. Morton, K. Moelmer, and P. Bertet, Phys. Rev. X **7**, 041011 (2017).
[14] S. Barzanjeh, D. P. Divincenzo, and B. M. Terhal, Phys. Rev. B **90**, 134515 (2014).
[15] N. Didier, A. Kamal, W. D. Oliver, A. Blais, and A. A. Clerk, Phys. Rev. Lett. **115**, 093604 (2015).
[16] L. C. G. Govia and A. A. Clerk, New J. Phys. **19**, 023044 (2017).
[17] N. Didier, J. Bourassa, and A. Blais, Phys. Rev. Lett. **115**, 203601 (2015).
[18] S. Hacohen-Gourgy, L. S. Martin, E. Flurin, V. V. Ramasesh, K. B. Whaley, and I. Siddiqi, Nature (London) **538**, 491 (2016).
[19] J. B. Hertzberg, T. Rocheleau, T. Ndukum, M. Savva, A. A. Clerk, and K. C. Schwab, Nat. Phys. **6**, 213 (2010).
[20] J. Suh, A. J. Weinstein, C. U. Lei, E. E. Wollman, S. K. Steinke, P. Meystre, A. A. Clerk, and K. C. Schwab, Science **344**, 1262 (2014).
[21] F. Lecocq, J. B. Clark, R. W. Simmonds, J. Aumentado, and J. D. Teufel, Phys. Rev. X **5**, 041037 (2015).
[22] See Supplemental Material at http://link.aps.org/supplemental/10.1103/PhysRevLett.120.040505 for experimental details and theoretical analyses of higher-order effects. Includes Refs. [23,24].
[23] A. A. Clerk and D. W. Utami, Phys. Rev. A **75**, 042302 (2007).
[24] C. W. Gardiner and P. Zoller, *Quantum Noise* (Springer, Heidelberg, 2004).
[25] H. Paik, D. I. Schuster, L. S. Bishop, G. Kirchmair, G. Catelani, A. P. Sears, B. R. Johnson, M. J. Reagor, L. Frunzio, L. I. Glazman, S. M. Girvin, M. H. Devoret, and R. J. Schoelkopf, Phys. Rev. Lett. **107**, 240501 (2011).
[26] F. Mallet, M. A. Castellanos-Beltran, H. S. Ku, S. Glancy, E. Knill, K. D. Irwin, G. C. Hilton, L. R. Vale, and K. W. Lehnert, Phys. Rev. Lett. **106**, 220502 (2011).
[27] E. Flurin, N. Roch, F. Mallet, M. H. Devoret, and B. Huard, Phys. Rev. Lett. **109**, 183901 (2012).
[28] B. Yurke, S. L. McCall, and J. R. Klauder, Phys. Rev. A **33**, 4033 (1986).
[29] C. Macklin, K. O'Brien, D. Hover, M. E. Schwartz, V. Bolkhovsky, X. Zhang, W. D. Oliver, and I. Siddiqi, Science **350**, 307 (2015).
[30] S. Boutin, D. M. Toyli, A. V. Venkatramani, A. W. Eddins, I. Siddiqi, and A. Blais, Phys. Rev. Applied **8**, 054030 (2017).
[31] S. Puri and A. Blais, Phys. Rev. Lett. **116**, 180501 (2016).
[32] C. W. Gardiner, Phys. Rev. Lett. **56**, 1917 (1986).
[33] H. Le Jeannic, A. Cavailì Es, K. Huang, R. Filip, and J. Laurat, arXiv:1707.06244.
[34] T. Walter, P. Kurpiers, S. Gasparinetti, P. Magnard, A. Potočnik, Y. Salathé, M. Pechal, M. Mondal, M. Oppliger, C. Eichler, and A. Wallraff, Phys. Rev. Applied **7**, 054020 (2017).
[35] K. M. Sliwa, M. Hatridge, A. Narla, S. Shankar, L. Frunzio, R. J. Schoelkopf, and M. H. Devoret, Phys. Rev. X **5**, 041020 (2015).
[36] J. Kerckhoff, K. Lalumière, B. J. Chapman, A. Blais, and K. W. Lehnert, Phys. Rev. Applied **4**, 034002 (2015).
[37] B. Levitan, Master's thesis, McGill University, 2015, digitool.library.mcgill.ca/thesisfile138943.pdf.
[38] A. Metelmann and A. A. Clerk, Phys. Rev. X **5**, 021025 (2015).
[39] F. Yan, S. Gustavsson, A. Kamal, J. Birenbaum, A. P. Sears, D. Hover, T. J. Gudmundsen, D. Rosenberg, G. Samach, S. Weber, J. L. Yoder, T. P. Orlando, J. Clarke, A. J. Kerman, and W. D. Oliver, Nat. Commun. **7**, 12964 (2016).